Energy & Buildings 277 (2022) 112578

Contents lists available at ScienceDirect

Energy & Buildings

journal homepage: www.elsevier.com/locate/enb

An experimental investigation on the radiant cooled wall's heat transfer characteristics in a fully conditioned real-sized living environment

Aliihsan Koca [a], Yakup Karakoyun [b,*], Ozgen Acikgoz [c], Mustafa Dogu [d], Ahmet Selim Dalkilic [c]

[a] Department of Mechanical Engineering, Faculty of Mechanical Engineering, Istanbul Technical University (ITU), Istanbul 34437, Turkey
[b] Department of Mechanical Engineering, Engineering Faculty, Hakkari University, Hakkari 30000, Turkey
[c] Department of Mechanical Engineering, Faculty of Mechanical Engineering, Yildiz Technical, University (YTU), Istanbul 34349, Turkey
[d] Mir Arastirma ve Gelistirme A.S., Istanbul 34220, Turkey

ARTICLE INFO

Article history:
Received 14 September 2022
Revised 9 October 2022
Accepted 13 October 2022
Available online 18 October 2022

Keywords:
Radiant wall
Radiant ceiling
Radiant floor
Heat transfer coefficient
Radiant cooling

ABSTRACT

Radiant wall applications have been favored compared to floor and ceiling ones owing to their advantages. In the current work, the heat transfer characteristics of a radiant cooled wall, which are heat fluxes, and heat transfer coefficients, have been experimentally investigated by altering supplied water temperatures and using proper reference temperatures in a fully conditioned real-sized test chamber where the obstacles such as unrealistic room sizes and insufficient air conditioning processes have been eliminated. Detailed methodology for the determination of reference temperature, used thermocouples' locations, and heat gains were revealed. As a result, investigated radiant cooled wall's average total, radiative, and convective heat transfer coefficients were determined as 7.83, 5.14, and 2.57 W/m^{2}K, in turn. 67 % of the total heat transfer rate in the mean was found to belong to radiation. Furthermore, novel empirical correlations on the total, radiative, and convective heat transfer coefficients were derived with the mean squared errors of 99 %, 98 %, and 99 %, respectively. There is no experimental investigation on radiant wall cooling excluding authors' previous publications. Finally, a detailed measured and calculated dataset, obtained from the third investigation on the radiant cooling wall system in open sources, was presented for the sake of other researchers.

© 2022 Elsevier B.V. All rights reserved.

1. Introduction

One of the most important issues to create a sustainable society is decreasing continuously increasing energy consumption by the way of properly defined energy usage policies. As the researchers reported [1–3], the proportion of residential energy usage has reached around 40 % of the global energy consumption. Thus, any decrease in energy consumption in the building sector can lead to a reduction in energy consumption globally. A possible path of decreasing energy consumption in a residential area is utilizing a system that benefits from low-temperature sources whose temperature is close to the indoor temperature. The low-temperature difference between indoor air and the thermal unit provides high thermal comfort to occupants because of lower air movements as well as higher proportions of radiation heat transfer (HT) in total, this also brings about diminishing energy consumption. The term clarifying such a system is low-temperature heating and high-temperature cooling application, which operate up to 40 °C in heating mode and up to 20 °C in cooling mode, respectively [4]. Operation up to the given temperatures induces an opportunity to employ those systems integrated with renewables, such as recovery and solar systems for heating mode, and heat pumps for cooling mode [5].

Radiant heating and cooling systems that use the room surfaces (wall, floor, and ceiling) to condition indoor air are low-temperature heating and high-temperature cooling applications. These systems come up with features embracing above mentioned advantages of low-temperature heating and low-temperature cooling. Additionally, radiant systems cause lower exergy destruction values and thus provide a better comfort condition in buildings thanks to diminishing natural convection currents, also radiative HT becomes the outweighing HT phenomenon via instrumenting the wide surfaces related to heat emitter or absorbers. Decreasing peak loads is another feature of those systems that contributes to total energy consumption positively. In open sources radiant systems come front with the dominant HT mechanism being radiation with more than 50 % of total HT [6,7], occurring between the conditioned surface and its environs. Recently, radiant heating and cooling applications are being desirable because of

* Corresponding author.
E-mail address: yakupkarakoyun@hakkari.edu.tr (Y. Karakoyun).

https://doi.org/10.1016/j.enbuild.2022.112578
0378-7788/© 2022 Elsevier B.V. All rights reserved.

Nomenclature

A	Area (m^2)
c_p	Specific heat at constant pressure (J/kgK)
$F_{\varepsilon_{s-j}}$	Radiation interchange factor
F_{s-j}	Angle factor between radiant surface and j-surface
h_c	Total heat transfer coefficient (W/m^2K)
h_r	Radiative heat transfer coefficient (W/m^2K)
h_t	Convective heat transfer coefficient (W/m^2K)
$\dot{m}_w$	Water mass-flow rate (kg/m^3)
Q_c	Convective heat transfer rate (W)
Q_g	Backside heat transfer rate (W)
Q_n	Total net heat transfer rate (W)
Q_r	Radiative heat transfer rate (W)
Q_t	Total net heat transfer rate (W)
$\dot{q}_c$	Convective heat-flux (W/m^2)
$\dot{q}_g$	Backward heat-flux (W/m^2)
$\dot{q}_r$	Radiant heat-flux (W/m^2)
$\dot{q}_t$	Total heat-flux (W/m^2)
$\dot{q}_n$	Total net heat-flux (W/m^2)
T_a	Average air temperature (°C)
T_{AUST}	Area-weighted average unconditioned surface temperature (°C)
T_{out}	Rear side temperature of the west wall (°C)
T_{ins}	Rear side temperature of the panel (°C)
T_j	j-surface temperature (°C)
T_{op}	Operative temperature (°C)
T_s	Average surface temperature (°C)
T_w	Water temperature (°C)
U	Total heat transfer coefficient for the wall (W/m^2K)
w_R	Error rate
ε	Emissivity
σ	Stefan-Boltzmann constant (W/m^2K^4)

Abbreviations

CFD	Computational Fluid Dynamics
HT	Heat Transfer
HTC	Heat Transfer Coefficient
HVAC	Heating Ventilating Air Conditioning
MRT	Mean Radiant Temperature
VOL	Volume

their distinguishing characteristics. The advantages of implementing the radiant systems compared to other air conditioning systems have been performed considering the thermal comfort and indoor air quality [8–10], response time [11], draft risk [10,12], and energy performance parameters [8,10,12–14] in several studies.

As it is mentioned before, radiant heating and cooling applications use their surfaces to condition the indoor environment, including the wall surfaces. To ascertain the advantages or disadvantages of utilizing radiant wall heating/cooling systems in comparison to other air conditioning applications various experimental and numerical works have been conducted. Oravec et al. [15] conducted numerical work to compare the different types of radiant systems including radiant wall heating systems in terms of thermal performance, energy storage, required radiant surface, and building cost. One of the outcomes of the investigation was that the implementation of the radiant wall system, especially in retrofitting structures, did not necessitate a significant modification in building structures. It was also concluded that the cost of installation of a radiant wall system was lower than the other examined radiant systems due to the simplicity of the installation process. The disadvantage of utilizing a radiant wall system was given as the possibility of system destruction in the situation of intervention.

According to a guidebook on low-temperature heating and high-temperature cooling systems published by REHVA [4], in the comparison of radiant heating and cooling systems with respect to their heating and cooling capacities, the cooling capacity of radiant walls is higher than the radiant floors but lower than the cooled ceilings, whereas the heating capacity of radiant walls is extremely greater than the other radiant surfaces. Even though Vangtook and Chirarattananon [16] stated that implementing radiant wall/ceiling cooling provides thermal comfort in hot climates, the authors have drawn attention to the thermal capacity of cooling systems that are easily affected by obstacles near the surfaces, which diminish the HT from the surfaces. Krajcik et al. [17] reviewed some studies on total heat transfer coefficients (HTCs), between heated/cooled radiant surfaces and living environment, pertaining to radiant heating and cooling applications, and deduced that the total HT coefficient was lesser for a cooled radiant wall than that for a cooled radiant ceiling. A similar deduction was also derived for radiant wall heating against floor heating systems. In addition, the authors also indicated that there existed the risk of having a thermally non-homogenous living environment in the case of the installation of a radiant wall that has an insufficient radiant surface.

Besides the studies concerning the comparison of the strengths and weaknesses of utilizing radiant wall heating and cooling applications with respect to other air conditioning systems, there exist numerous numerical and experimental works on wall systems in the view of the energy performances when coupled with auxiliary systems, equipment, or construction materials, and thermal comfort. With the aspect of thermal comfort, according to studies [16,18–22], it was revealed that radiant wall heating and cooling applications could improve the thermal comfort of the indoor environment due to low velocities of air particles, having less draft risk, adjusting circulating fluid temperature, and providing a uniform indoor air temperature distribution. Moreover, Vangtook and Chirarattananon [23] revealed that radiant wall cooling applications could be implemented in indoor environments that have a low amount of heat gain. Besides the thermal comfort studies, works regarding the energy performance of radiant wall heating and cooling systems also have been conducted. As it is indicated before, radiant heating and cooling applications may be categorized as one of the low-temperature heating and high-temperature cooling applications that bring an opportunity of coupling these systems with low-quality energy sources, such as heat pumps, roof-type solar heating applications, waste heat systems, etc. The studies [24–27] concluded that the energy performance of radiant wall heating and cooling applications that condition the living environments had high exergy efficiency performance, especially when coupled with renewable energy sources [28].

Based on the literature survey on radiant heating and cooling applications, it is seen that they have been commonly implemented because of their high thermal comfort ability and energy-saving capability. In addition to the studies on the thermal comfort and energy consumption performance of radiant wall heating and cooling systems, several works also have been done to investigate the HT characteristics of radiant wall systems, including heat fluxes, HTCs, temperate distributions over surfaces

and indoor air, etc. Apart from the other indoor air conditioning systems, radiant systems condition the living environment at quite high proportions of radiation in total HT, which occurs between conditioned surfaces and their surroundings. The HTCs of radiant systems pertaining to radiation and convection are utilized to determine the HT that takes place by those mechanisms. In addition to the determination of HT via such systems, HTCs are also utilized in system designing processes. Thus, assigning the accurately defined HTCs (total, radiative, and convective) in the design stage of radiant systems has a crucial impact on avoiding high energy consumption. Furthermore, it should be emphasized that in the calculation processes of the HTCs, the reference temperatures have an important role. Generally, operative temperature, air temperature of the indoor environment, and the area-weighted average temperature of unconditioned surfaces have been used in the calculation processes of the total, convective, and radiative HTCs.

When analyzing the studies and standards on radiant wall heating and cooling applications that propose the HTCs or correlations in the open sources, it can be seen a noticeable discrepancy among the suggested HTCs. In the case of evaluating total HTCs, EN 15377 [29], EN 1264 [30], and REHVA [4] standards proposed a single value of total heat transfer coefficient both for radiant wall heating and cooling systems as 8 W/m^{2}K. On the other hand, in the investigations conducted by Koca et al. [31,32], Acikgoz, et al. [33], and Karabay et al. [18], the proposed values of total HTCs are in the interval of 7.72–11.22 W/m^{2}K valid for only radiant wall heating systems. Regarding the radiative HTCs belonging to radiant wall heating applications, it may be pointed out that there exists a consensus on the values that vary in a quite small range of 4.83–6.25 W/m^{2}K, and commonly a constant value (5.5 W/m^{2}K) is proposed. Different from the recommendations on radiative and total HTCs, both correlations and constant values have been proposed in studies to calculate the convective HTCs. While the equations suggested by ASHRAE [34], Alamdari and Hammond [35], and Churchill and Chu [36] have been derived from vertical plate experiments, the correlations proposed by ASHRAE [37], Awbi and Hatton [38], Khalifa and Marshall [39], and Açıkgöz [40] have been acquired by real-sized wall/enclosure experiments as separated approaches. In the suggested correlations, the common parameter is the temperature difference between examined surface and indoor air for both of them. In addition, the studies performed in real-sized rooms on the calculation of convective HTCs pertaining to radiant heating wall applications proposed constant values that vary in the interval of 2.40–2.70 W/m^{2}K. It should be noted that the entire proposed coefficients are obtained by the experiments on radiant heated walls. When the case is a radiant cooled wall, as Shinoda et al. [41] also stated, the only experimental study that concerns the heat transfer characteristics belonging to the radiant wall cooling application was conducted by Acikgoz and Kincay [42]. The authors proposed the values of 8.1, 4.3, and 2.7 W/m^{2}K for the total, radiative, and convective HTCs, respectively. Recently, second work on the calculation of HT characteristics of radiant cooled walls in a real-sized fully conditioned both inside and outside spaces has been performed by Koca [43]. In his work, the HTCs of 8.25, 5.52, and 2.41 W/m^{2}K were derived from the quite accurate experiments belonging to the total, radiation, and convection, correspondingly. Main difference of his study from the current investigation was the usage of two different radiant panels to examine their thermal performances. It is concluded that the thermal capacity of the aluminum panel was found to be higher than the conventional one.

In comparison to radiant ceiling and floor systems, the application of radiant walls is easier and can lead reduction in energy consumption in specified conditions. For example, energy efficiency is affected by the thermal insulation enabled by radiant panels positively. Conventionally, investigations on these subjects have mostly focused on floors or ceilings. The application of radiant wall usage is considered a promising approach based on the various works in open sources contrasted to floor and ceiling ones. Moreover, in spite of the common use of radiant heating and cooling systems in living environments, problems regarding the prediction of thermal load for the period of the design stage still continue. In the current investigation, experimental data were taken to examine and contrast the HT characteristics of the room, heat fluxes, HTCs, and temperature distribution both over the surfaces and air, having embedded cold water pipes that acted as a radiant cooling wall application. Encompassing the entire tests, the temperature of the operating fluid delivered to the hydronic circuit was altered. When the steady-state regime was reached, with one-minute time intervals the heat fluxes were evaluated. Moreover, entire significant factors, the reference temperature determination height and the method for determination of heat gain, are revealed comprehensively. The current study should be considered as a continuation of researchers' previous publications [42,43] in the literature. Koca et al. [18,20] studied radiant wall heating in detail and stated that most of the existing investigations regarding the HT characteristics of radiant applications concentrated on heating. Apart from the radiant cooling studies conducted by Acikgoz and Kincay [42] and Koca [43], there is no experimental investigation present in the open sources. For that reason, the current investigation of these researchers is expected to be a pioneer one in the near future. It should be noted that thermal works conducted in real-sized rooms are mainly performed for the aim of either investigating thermal comfort or researching HT characteristics of radiant systems. In general, practical works related to these issues have problematic points with room sizes and the air conditioning process of rooms' outer environment, it should be noted that given obstacles have been eliminated by having real sized and well-conditioned both room and its outer surrounding. In the light of the indicated information above, the existing experimental investigation aims to fill the gap on the radiant wall cooling subject.

2. Experimental methodology

2.1. The layout of the experimental chamber

The experimental chamber was built to simulate a radiant cooling application with variable boundary conditions, as indicated in Table 1. The climatic chamber used in the practical works was built to accurately replicate the possible living environment and attributes of a full-sized chamber (illustrated in Fig. 1). As illustrated in Fig. 1 and Fig. 2, the experiment room is composed of parts that are the facade (vol. 2), the floor (vol. 3), the ceiling (vol. 4), and the investigated region (vol. 1). According to BS EN 14037-5 [44] and EN 1264-5 [30] standards, radiant cooling panels were installed in the examined area having a floor area of 24 m^2 and an inner height of 3 m. The walls are constructed with steel-out layers and core polyurethane insulation. In some investigations, the temperature difference between surface and indoor air, and conditioned surface sizes are described as important factors for the calculation of convective HT. In order to attain more accurate and stable convective HTCs, a real-sized test room has been constructed controlling its outer surroundings with an air conditioning system.

Mechanical air conditioners were utilized to sustain the thermal environment of the surroundings to offer appropriate boundary conditions in the experimental area (Fig. 2). To assess the emissivity of the room surfaces and cooled radiant walls, which were utilized to calculate radiant HT, a calibrated temperature sensor and a thermal camera were employed. Using thermos-elements, the surface temperature was observed. Then, in the pyrometer setup, the

Table 1
Zone control parameters.

	Volume 1	Volume 2	Volume 3	Volume 4
Temperature Span	+30C/0C	+40C/−10C	+30C/0C	+40C −10C
Temperature Tolerance	± 0.5C	± 0.5C	± 0.5C	± 0.5C
Humidity Range	–	%35/%85 RH	–	–
Humidity Control Steps	–	%1	–	–
Humidity Tolerance	–	± % 0.5 RH	–	–
Air Velocity	–	0.5 – 5 m/s	–	–

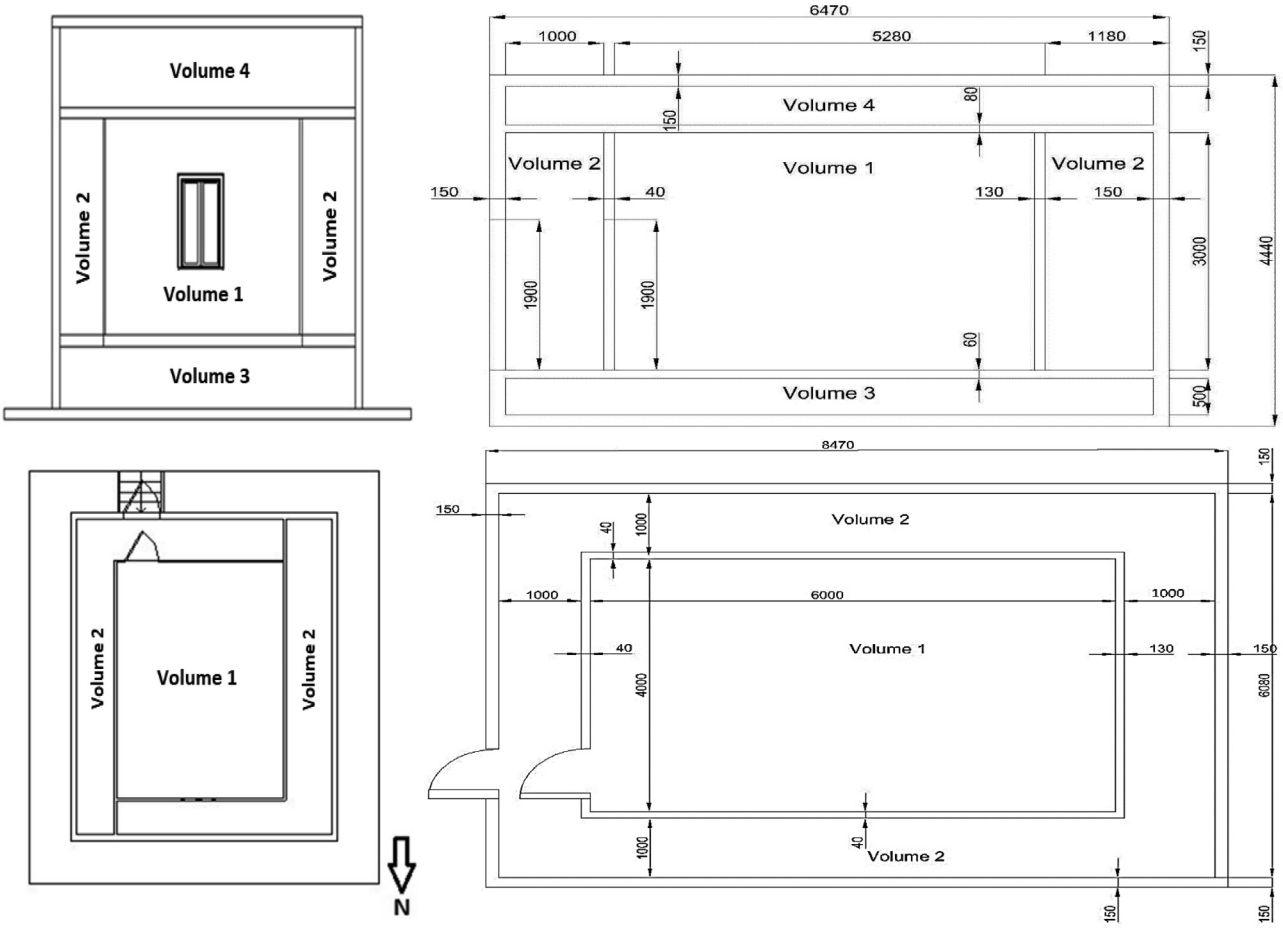


Fig. 1. Dimensions and general perspectives of the testing facility.

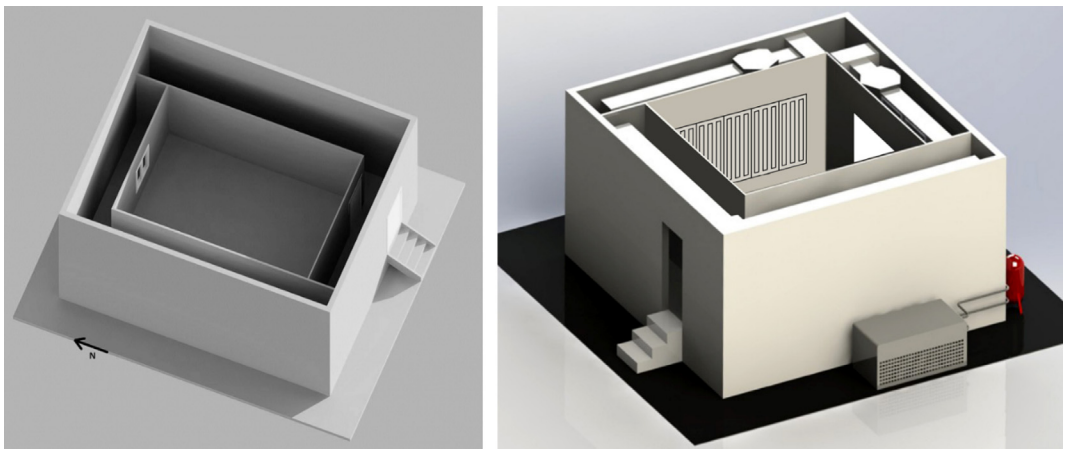


Fig. 2. 3-D illustration of the experimental room.

surface emissivity was altered to achieve the identical temperature of the surface being inspected as that previously obtained employing thermos-elements [45,46]. The experimental set-up complies with the fundamental requirements of ASHRAE Standard 138 in terms of both its physical parameters and thermophysical parameters [47].

2.2. Radiant system structure

Radiant cooling panels comprised of four components were constructed for this study: a plasterboard, an aluminum foil layer, a cooling pipe, and insulation. The tube coil is located in the plasterboard which is 15 mm thick, while the insulating material is 50 mm thick. The aluminum foil, placed between the plasterboard and the insulation that covers the serpentine groove layer, was employed to decrease the surface temperature and ensure uniform surface temperature distribution. The serpentine pipe is composed of Polyethylene of Raised Temperature Resistance with a 12 mm diameter and 150 mm pipe spacing. A thermally insulating layer comprised of Extruded Polystyrene with a thermal conductivity value of approximately 0.04 W/mK at 20 ℃ was employed (Fig. 3).

The testing area was constructed with 5 radiant wall cooling panels (1 m × 2.2 m) mounted over the whole western façade (Fig. 4).

2.3. The hydronic circuit of the radiant cooling wall application

The experimental apparatus consisted of a hydronic system providing the radiant cooling system with a suitable inlet water flow rate and temperature. The hydraulic circuit, as shown in Fig. 5, consists basically of the entering water to the system by means of the tank (a cooling unit was implemented to generate the cooled water), a 4-way valve permitting the inlet water temperature to be altered by combining the supply and return tube line, a 3-way valve that keeps the mass-flow rate of the water at the right rate, and an ultrasonic flow-meter that tracks the mass flow rate and gives data. The cooled water is then routed to the collector and, eventually, to the radiant cooling facility to proceed with the HT process. Following the completion of the circuit in the panel, the water returns to the 4-way valve along the return line and, if necessary, is brought together with water from the tank (to change the necessary temperature of the water). The hydraulic pipeline was thoroughly isolated from heat gain. More information about the hydraulic system is available in [48].

2.4. The measurement apparatus

To determine the transferred heat through a conditioned surface, the result acquired merely indicates the HT at the location it is mounted, thus its capability to present the total HT rate should be examined. Additionally, surface temperature and heat flux measuring devices change the surface circumstances and temperature of their location, which may lead to inaccurate measurements. Furthermore, their measurement accuracy is also affected by the establishment of proper contact during their installation to the surface. To cope with the indicated problems, the indoor air temperatures belonging to the experimental chamber were determined utilizing various thermos-elements in the test room. The measurements from vertically and horizontally oriented by these sensors resulted in a more stable and wide-scanned temperature area. Radiation preventers were covered on the thermocouples to avoid the influence of radiation.

The inner air temperatures (T_a) of the testing area were obtained by implementing 16 K-type thermos-elements (T_{a1}–T_{a16}) arranged horizontally and vertically in the test room (Fig. 6). A reliable and precise temperature pattern was realized from the observations performed in this way. To avoid the effects of radiation, radiation shields were put on the sensors. Two panels, one from the north wall and one from the west wall, were chosen as representative panels for detailed analysis. Table 2 displays the locations of the air temperature sensors throughout the area of investigation. The surface temperatures of the radiant surface were observed by applying six thermo-elements mounted on the surfaces of each panel (T_{s1}–T_{s6}) (Fig. 6). Those surface temperatures were averaged out for each test, and that temperature was used as the average temperature of the cooled surface (T_s).

According to ASHRAE Standard 55 [49], each unconditioned surface contains one surface thermo-element in the middle to compute the area-weighted uncooled/unheated mean surface temperature (T_{AUST}). Since the uncooled surfaces are composed of highly conductive material, it was decided to install a single surface thermo-element in the middle of them. In order to further support this assertion, the temperature distribution of the surfaces was measured using a thermal camera, and in every test case, a uniform surface temperature profile was seen over the surfaces. The temperature sensors were glued to the surfaces after being suitably coated with a thermal insulation layer. In addition, radiation shields were mounted on top of the thermos-elements to protect them from unanticipated radiation impacts. The air temperatures in every part were monitored and managed to keep track of and regulate the external climatic conditions, as well. The temperatures of the backside of the west-wall (T_{out}) of vol. 2 as well as the temperature of the back side of the sample panels (T_{ins}) were measured to calculate the heat transferred to the examined wall.

The operating temperature (T_{op}) was evaluated using a thermal comfort measurement apparatus (Fig. 7) positioned in the middle of the experimental zone.

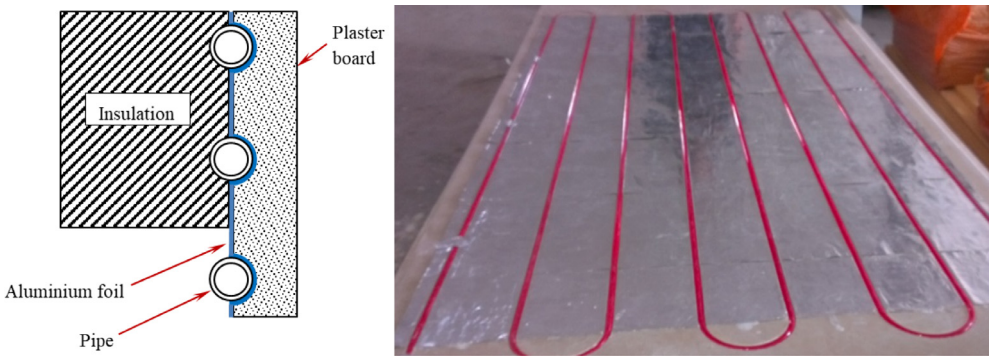


Fig. 3. Radiant wall panels.

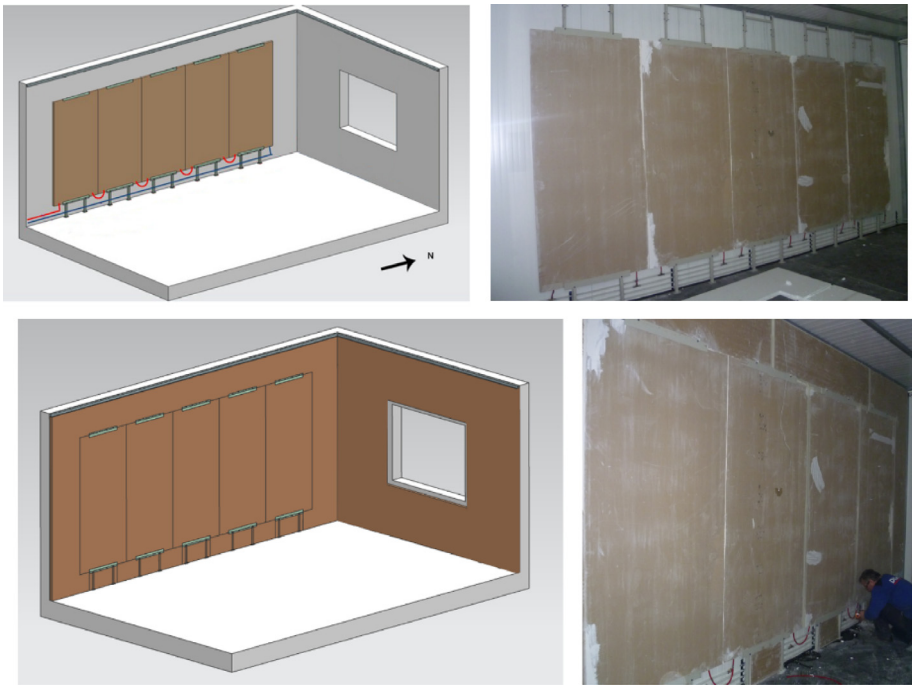


Fig. 4. The system configuration for cooled radiant walls.

For the relevant temperature range, which was between 10 °C and 20 °C, all thermos-elements were accurately calibrated. The calibration findings showed a proper straight tendency (R^2 < 0.990), within the ±0.1 °C precision interval (Fig. 8).

The mass-flow rate of the supplying water was measured employing an ultrasonic flowmeter with an error deviation of ±1 %. The water temperatures in the hydronic line were measured by utilizing the inlet and outlet of the cooling panels (T_{w1} and T_{w2}). To regulate and monitor the temperatures in the hydronic line, additional water temperature sensors were mounted at the buffer tank (T_{w4}), in between the pump and the four-way valve (T_{w3}), and at the inflow (T_{w5}) and outflow (T_{w6}) of the cooling unit (Fig. 5).

The CDMS (control and data monitoring system) for the surrounding volumes is completely distinct and autonomous from the CDMS for the volume-1 under examination. Evaluating a PLC device, CDMS accomplishes, among other items, the cooling unit, air handling device, pumps, and motorized valves in surrounding areas. The NI Labview© program was used to keep track of data gathered from the sensors in the testing zones. Further information related to the hydronic line exists in [45,46].

2.5. The experimental methodology

The primary goal of the current study was to investigate the HTCs of the radiant cooling application. Trustworthy tests were based on observations made in the real-scale testing facility described above. In each experiment, the relevant variables, including the water flow rate, were fixed to a particular value. During steady-state circumstances, measurements were performed according to EN 14240 [50]. Surface temperatures and water entering and exit temperatures in cooling panels were taken into consideration as indicators of the steady-state regime. In order to adjust the temperature of the inner surfaces of vol. 1, the surrounding volumes were held at predetermined boundary conditions until the requested temperatures (0.5 °C) were attained. To obtain the proper heat flow by means of the cooling application within the steady-state boundary regimes, the hydraulic process was initiated before collecting experimental data. Depending on the experimental situations and boundary conditions, steady-state criteria were fulfilled in 4–5 h, during which flow rates, supply water temperature, surface temperatures of uncooled surfaces and cooled panels, as well as indoor and enclosing volume air temperatures were relatively stable. Afterward, each run was undertaken. In order to maintain the radiant surfaces at the appropriate temperature prior to conducting the HT calculations, chilled water was provided to the cooling panels whereas the uncooled surface temperatures and interior air temperature changed relying on the cooling output of the wall panels.

The total cooling load of the radiant cooled panels was determined by monitoring the mass flow rate ($\dot{m}_w$), as well as the inlet water temperature (T_{w1}) and outlet temperatures (T_{w2}). In the final HTC computation, T_{op}, which was acquired practically by the thermal comfort apparatus—was used. The operative temperature, as ASHRAE 55 [49] proposed, is the weighted mean of the dry bulb air temperature and the average radiant temperature. The average of 16 air temperatures (T_{a1}–T_{a16}) distributed throughout the testing area was used to calculate convection HT. The temperature discrepancies between the exterior surface of the radiant walls (in which the examined wall panels (T_{out}) are mounted) and the backside of the representative wall panels (T_{ins}), along with the insulation thickness, the surface areas of each panel (A), and the U values of the wall structure, were used to compute the heat gain towards the cooling panels for each measurement time-step. This calculation was conducted for each test case to derive the net cooling power of the radiant system.

In addition, inside and outside zones' air temperatures, the temperature of all surfaces, the inlet and outlet water temperatures, and the mass-flow rates were observed, sustained, and gathered for every measurement interval (1 min). Experiments were run for about 12 h to verify that all essential variables attained steady-state and target levels, as well as to allow for adequate data storage. When the system reached a steady-state regime, the HTCs and heat-fluxes were calculated. The outcomes were derived from the mean values obtained during 30-minute periods where steady regimes were sustained. Measuring started when the temperatures of the cooling surface and indoor air steadied within a 0.1 K/min

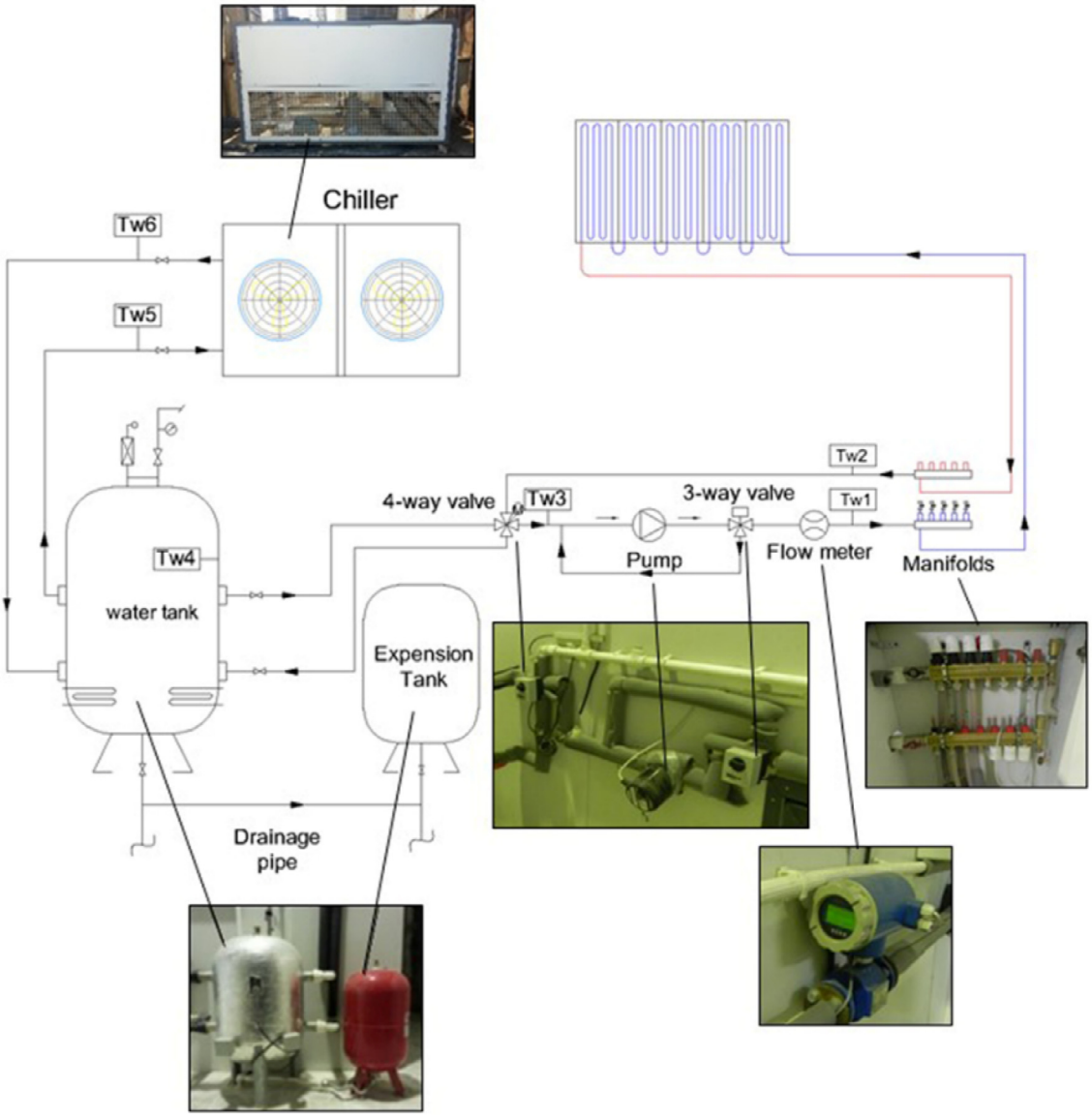


Fig. 5. Radiant cooling system configuration with hydraulic circuit.

interval. Convective HTCs (h_c), radiant HTCs (h_r), and total HTCs (h_t), were computed via data gathered and represented in the results and discussions part.

3. Calculation procedure

By and large, determined and suggested HTCs in the open sources pertaining to radiant systems require extensive insight into measurement techniques along with calculation methodology performed for all cases. Considering the relevant literature rigorously, one can notice differences in the dimensions of the examined room, the investigated surface of the chamber, the way of determination of transferred heat, where the reference temperature point is selected, and whether ventilation is present or not, exist. According to Shinoda et al. [41], HTCs proposed by a great number of researchers display discrepancies despite the surrounding environment being the same, also in case the given HTCs in widely resorted databases and standards are set against data of those investigations. One possible reason for differences in total HTCs can be accounted for by the differences in convective streams and their strength in different investigations. It can be concluded that choosing a suitable HTC for an application should be subject to an in-depth examination. Impactful ingredients that are the position of the measurement points, as well as HT rates' determination procedure, are deficient in a great number of studies and therefore it is seen that sufficient clarification on outlining the surrounding environment does not exist. All points indicated in previous lines were taken into consideration in the current work.

3.1. Conservation of energy

The following equation describes the overall rate of HT to the cooled radiant panels (Q_t) because of convection between air and panel surface (Q_c), net thermal radiation from the unconditioned surroundings (Q_r), and heat transmitted by conduction through the rear of the cooled wall (Q_g):

$$Q_t = Q_r + Q_c + Q_g \tag{1}$$

The total net HT by the radiant cooled wall was determined via heat-flux ($\dot{q}_n$) through the radiant cooled wall and was found by excluding the heat-gain ($\dot{q}_g$) out of total heat-flux ($\dot{q}_t$):

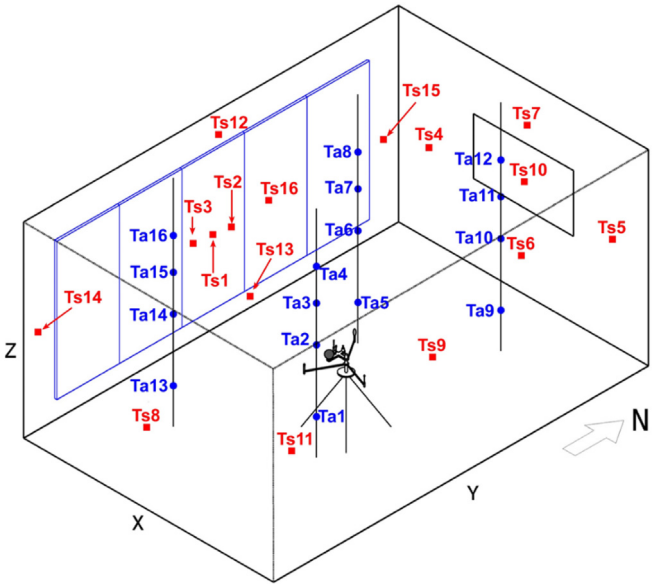


Fig. 6. Arrangement of temperature sensors.

$$\dot{q}_n = \frac{\dot{m}_w C_p \Delta T_w}{A} - \dot{q}_g \tag{2}$$

where, $\dot{q}_t$ was determined using the temperature difference between the water inlet (T_{w1}) and outlet temperature (T_{w2}) of the hydronic circuit by multiplying the water mass-flow rate ($\dot{m}_w$) and the specific heat (c_p), and dividing by surface area A (m^2) of the cooled panel. Furthermore, $\dot{q}_g$ (W/m^2) is the heat-gain by conduction through the rear surfaces of radiant cooled panels and is calculated as:

$$\dot{q}_g = -k_{ins}\left.\frac{dT}{dx}\right]_{ins} \tag{3}$$

In Eq. (3), T_{ins} (K) can be defined as the rear surface temperature of the radiant cooled panels located at starting point of the insulation, T_{out} (K) is the temperature at the outer surface of the wall (in Vol. 2), and U_{ins} (W/m^2K) is the total HTC of the entire conduction layers circuit of the wall.

The net heat-flux of the radiant wall cooling application extracted from the experimental chamber, consisting of convective and radiative heat fluxes, is defined as follows:

$$\dot{q}_n = \dot{q}_r + \dot{q}_c \tag{4}$$

Moreover, the net total heat-flux, comprising convective and radiative heat fluxes, is presented:

$$h_t(T_{op} - T_s) = h_r(T_{aust} - T_s) + h_c(T_a - T_s) \tag{5}$$

In this equation, T_a (K) denotes the mean air temperature, T_{AUST} (K) symbolizes the area-weighted Average-Uncooled/Unheated Surface-Temperature, h_c (W/m^2K) is the convective, and h_r (W/m^2K) is the radiative HTC.

3.2. Determination of heat transfer coefficients

The radiative HTC is found employing the T_{AUST} and using the calculated angle factors between the radiant surfaces [51]. It should be noted that, for every unconditioned surface, a uniform temperature dispersal was obtained:

$$T_{AUST} = \sqrt[4]{\sum_{j=1}^{n}(F_{s-j}\,T_j^4)} \tag{6}$$

$$F_{\varepsilon_{s-j}} = \frac{1}{[(1-\varepsilon_s)/\varepsilon_s] + (1/F_{s-j}) + (A_s/A_j)[(1-\varepsilon_j)/\varepsilon_j]} \tag{7}$$

$$F_{s-j} = \frac{1}{A_i}\int_{A_i}\int_{A_j}\frac{\cos\theta_i \cos\theta_j}{\pi R^2}\,dA_i\,dA_j \tag{8}$$

To determine the radiant heat-flux ($\dot{q}_r$) between the radiant cooled wall and its surrounding surfaces, Eq. (9) was utilized, whereas the Eq. (10) was implemented to obtain the radiative HTC:

$$\dot{q}_{r=}\sigma\sum_{j=1}^{n}F_{\varepsilon_{s-j}}\left(T_s^4 - T_j^4\right) \tag{9}$$

$$h_r = \frac{\dot{q}_r}{T_{AUST} - T_s} = \frac{\sigma\sum_{j=1}^{n}F_{\varepsilon_{s-j}}\left(T_s^4 - T_j^4\right)}{T_{AUST} - T_s} \tag{10}$$

T_s symbolizes the mean temperature of six temperature measurement points ($T_{s1} - T_{s6}$) spotted on the cooled radiant walls.

The angle factors in Eq. (7) were obtained by computationally evaluating the indicated equations in Matlab©. Fig. 9 demonstrates the numbered surfaces in vol. 1, and the outcomes of these computations are given in Table 3.

Throughout the calculations, 0.80 was the emissivity of the radiant cooled wall, and 0.90 was the value for unconditioned surrounding surfaces. Those values were computed by experimental measurements by merging surface temperature measurement and thermographic imagery. 3-D Matlab© code was utilized to calculate the radiative HT between all surfaces of the chamber.

Eq. (11) was employed to determine the total HTC (h_t), in which the net total heat-flux ($\dot{q}_n$) can be identified as the summation of convective ($\dot{q}_c$) and radiative ($\dot{q}_r$) heat fluxes.

$$h_t = \frac{\dot{q}_n}{T_s - T_{op}} \tag{11}$$

Utilizing the mean air temperatures (T_{a1} -T_{a16}), the convective HTC between the room air and the cooled wall surface are calculated in the following equations.

$$\dot{q}_c = \dot{q}_n - \dot{q}_r \tag{12}$$

$$h_c = \frac{\dot{q}_c}{T_a - T_s} \tag{13}$$

Table 2
Placement of air termo-elements.

Sensor	X_axial	Y_axial	Z_axial	Sensor	X_axial	Y_axial	Z_axial
T_{a1}	250	250	10	T_{a9}	200	500	10
T_{a2}	250	250	110	T_{a10}	200	500	110
T_{a3}	250	250	170	T_{a11}	200	500	170
T_{a4}	250	250	250	T_{a12}	200	500	250
T_{a5}	150	400	10	T_{a13}	100	100	10
T_{a6}	150	400	110	T_{a14}	100	100	110
T_{a7}	150	400	170	T_{a15}	100	100	170
T_{a8}	150	400	250	T_{a16}	100	100	250



Fig. 7. Operative temperature measurement device.



Fig. 8. Calibration equipment.

3.3. Uncertainty examinations

Various inaccuracies that may occur during the course of the experiment can affect the precision of the study. To diminish the uncertainty of the experimental findings, before choosing the interval of measurement equipment, an error examination should be conducted. Measuring the most remarkable parameter with more accuracy will provide the uncertainty of results to be lower. The uncertainty analysis method, which Holman first presented [52], is one of the error analysis techniques that is most frequently employed for experimental research. Equation (14) may be implemented to get the margins of error w_r for each individual parameter used in investigations. Errors might take place in two ways throughout the data evaluation process. There are errors that cannot be avoided because of the design of the experimental facility and the measuring equipment, and there exist errors that cannot be avoided because of the carelessness of the experimenter [52].

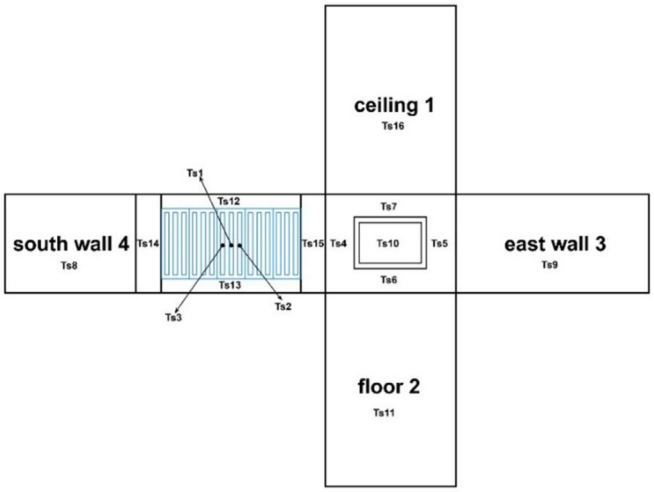


Fig. 9. Surfaces numerated taking place in vol. 1.

$$w_R = \pm\left[\left(\frac{\partial R}{\partial x_1}w_1\right)^2 + \left(\frac{\partial R}{\partial x_2}w_2\right)^2 + \ldots.\left(\frac{\partial R}{\partial x_n}w_n\right)^2\right]^{1/2} \quad (14)$$

In which R denotes the obtained value by means of experimental methods and x is the independent variant that affects R.

The total HT rate uncertainty was formulated as having:

$$\dot{q}_t = \frac{\dot{m}_w C_p (T_{w2} - T_{w1})}{A} \quad (15)$$

$$\dot{m}_w = \rho \dot{\vartheta}_w \quad (16)$$

$$w_{\dot{m}_w} = \pm\left[\left(\frac{\partial \dot{m}_w}{\partial \dot{\vartheta}_w}w_{\dot{\vartheta}_w}\right)^2\right]^{1/2} \quad (17)$$

$$w_{\dot{q}_t} = \pm\left[\left(\frac{\partial \dot{q}_t}{\partial \dot{m}_w}w_{\dot{m}_w}\right)^2 + \left(\frac{\partial \dot{q}_t}{\partial T_{w1}}w_{T_{w1}}\right)^2 + \left(\frac{\partial \dot{q}_t}{\partial T_{w2}}w_{T_{w2}}\right)^2\right]^{1/2} \quad (18)$$

The following formula can be used to calculate the uncertainty within the net rate of HT through the cooling panel:

$$\dot{q}_n = \dot{q}_t - \dot{q}_g \quad (19)$$

$$\dot{q}_g = U_w (T_{out} - T_{ins}) \quad (20)$$

$$w_{\dot{q}_g} = \pm\left[\left(\frac{\partial \dot{q}_g}{\partial T_{out}}w_{T_{out}}\right)^2 + \left(\frac{\partial \dot{q}_g}{\partial T_{ins}}w_{T_{ins}}\right)^2\right]^{1/2} \quad (21)$$

$$w_{\dot{q}_n} = \pm\left[\left(\frac{\partial \dot{q}_n}{\partial \dot{q}_t}w_{\dot{q}_t}\right)^2 + \left(\frac{\partial \dot{q}_n}{\partial \dot{q}_g}w_{\dot{q}_g}\right)^2\right]^{1/2} \quad (22)$$

Table 3
Determined angle factors.

Surfaces	1	2	3	4	5	6	7	8	9	10	11	12	13	14	15	16
1		0.340	0.200	0.130	0.0130	0.120	0.0130	0.0470	0.0090	0.0120	0.0390	0.0180	0.0080	0.0080	0.0220	0.0220
2	0.340		0.200	0.130	0.0130	0.130	0.0130	0.0160	0.0290	0.0330	0.0140	0.0170	0.0090	0.0090	0.0240	0.0240
3	0.270	0.270		0.130	0.0140	0.130	0.0140	0.0280	0.0160	0.0200	0.0210	0.0150	0.0050	0.0240	0.0360	0.0140
4	0.260	0.260	0.200		0.0510	0.110	0.0030	0.0210	0.0120	0.0130	0.0160	0.0120	0.0070	0.0070	0.0160	0.0160
5	0.200	0.200	0.160	0.410		1.30e-7	7.20e-12	4.80e-9	1.90e-8	0.0040	0.0050	0.0040	0.0000	0.0030	0.0060	0.0030
6	0.260	0.280	0.220	0.120	1.80e-8		1.20e-7	3.10e-8	8.50e-9	0.0170	0.0180	0.0180	0.0100	0.0050	0.0160	0.0370
7	0.200	0.200	0.160	0.030	7.20e-12	9e-7		4.80e-9	1.90e-8	0.0370	0.0600	0.0120	0.2000	0.0010	0.0050	0.0900
8	0.450	0.150	0.200	0.100	2.90e-9	1.40e-7	2.90e-9		1.80e-14	0.0080	0.0320	0.0150	0.0050	0.0050	0.0130	0.0230
9	0.140	0.470	0.200	0.100	1.90e-8	6.20e-8	1.90e-8	3e-14		0.0260	0.0080	0.0130	0.0060	0.0050	0.0140	0.0250
10	0.160	0.430	0.160	0.090	0.0030	0.100	0.0300	0.0100	0.0210		4.40e-11	1.90e-8	3.520e-8	3.52e-8	9.73e-8	9.73e-8
11	0.420	0.150	0.170	0.080	0.0030	0.090	0.0410	0.0360	0.0050	3.70e-11		1.20e-8	3.10e-8	3.11e-8	1.90e-7	1.90e-7
12	0.280	0.260	0.180	0.090	0.0040	0.130	0.0110	0.0240	0.0120	2.20e-8	1.70e-8		1.50e-9	1.51e-9	1.39e-7	1.39e-7
13	0.190	0.210	0.080	0.080	0.0010	0.110	0.3030	0.0130	0.0090	6.60e-8	7e-8	2.30e-9		3.53e-12	2.29e-9	3.01e-8
14	0.190	0.210	0.440	0.080	0.0040	0.060	0.0020	0.0120	0.0070	6.60e-8	7e-8	2.30e-9	3.50e-12		1.67e-8	2.29E-9
15	0.240	0.270	0.290	0.090	0.0040	0.080	0.0040	0.0150	0.0090	8.20e-8	1.90e-7	9.70e-8	1.03e-9	7.52e-9		3.57e-9
16	0.240	0.270	0.110	0.090	0.0020	0.190	0.0610	0.0260	0.0170	8.30e-8	1.90e-7	9.70e-8	1.35e-8	1.03e-9	3.57e-9	

The radiation HTC and radiative HT rate uncertainty were described as follows:

$$\dot{q}_r = \sigma \sum_{j=1}^{n} F_{\varepsilon_{s-j}} \left(T_s^4 - T_j^4\right) \tag{23}$$

$$w_{\dot{q}_r} = \pm \left[\left(\frac{\partial \dot{q}_r}{\partial T_s} w_{T_s} \right)^2 + \left(\frac{\partial \dot{q}_r}{\partial T_{s1}} w_{T_{s_1}} \right)^2 + \cdots + \left(\frac{\partial \dot{q}_r}{\partial T_{16}} w_{T_{s16}} \right)^2 \right]^{1/2} \tag{24}$$

$$h_r = \frac{\dot{q}_r}{(T_{aust} - T_s)} \tag{25}$$

$$T_{aust} = \sqrt[4]{\sum_{j=1}^{n} F_{s-j} T_j^4} \tag{26}$$

$$w_{T_{aust}} = \pm \left[\left(\frac{\partial T_{aust}}{\partial T_{s1}} w_{T_{s1}} \right)^2 + \left(\frac{\partial T_{aust}}{\partial T_{s2}} w_{T_{s2}} \right)^2 + \cdots + \left(\frac{\partial T_{aust}}{\partial T_{s6}} w_{T_{s16}} \right)^2 \right]^{1/2} \tag{27}$$

$$w_{h_r} = \pm \left[\left(\frac{\partial h_r}{\partial \dot{q}_r} w_{\dot{q}_r} \right)^2 + \left(\frac{\partial h_r}{\partial T_{aust}} w_{T_{aust}} \right)^2 + \left(\frac{\partial h_r}{\partial T_s} w_{T_s} \right)^2 \right]^{1/2} \tag{28}$$

The uncertainty in the convection HTC and convection HT rate was defined in the following equations:

$$\dot{q}_c = \dot{q}_n - \dot{q}_r \tag{29}$$

$$w_{\dot{q}_c} = \pm \left[\left(\frac{\partial \dot{q}_c}{\partial \dot{q}_n} w_{\dot{q}_n} \right)^2 + \left(\frac{\partial \dot{q}_c}{\partial \dot{q}_r} w_{\dot{q}_r} \right)^2 \right]^{1/2} \tag{30}$$

$$h_c = \frac{\dot{q}_c}{(T_a - T_s)} \tag{31}$$

$$w_{h_c} = \pm \left[\left(\frac{\partial h_c}{\partial \dot{q}_c} w_{\dot{q}_c} \right)^2 + \left(\frac{\partial h_c}{\partial T_a} w_{T_a} \right)^2 + \left(\frac{\partial h_r}{\partial T_s} w_{T_s} \right)^2 \right]^{1/2} \tag{32}$$

The uncertainty of total HTC and total HT rate were expressed as given:

$$\dot{q}_n = h_t (T_{op} - T_s) \tag{33}$$

$$h_t = \frac{\dot{q}_n}{(T_{op} - T_s)} \tag{34}$$

$$w_{h_t} = \pm \left[\left(\frac{\partial h_t}{\partial \dot{q}_n} w_{\dot{q}_n} \right)^2 + \left(\frac{\partial h_t}{\partial T_{op}} w_{T_{op}} \right)^2 + \left(\frac{\partial h_t}{\partial T_s} w_{T_s} \right)^2 \right]^{1/2} \tag{35}$$

T_s in the previous equations is the average of the values of the six surface temperature sensors ($T_{s1} - T_{s3}$) positioned over the cooled panel:

$$T_s = \frac{T_{s1} + T_{s2} + T_{s3}}{3} \tag{36}$$

$$w_{T_s} = \pm \left[\left(\frac{\partial T_s}{\partial T_{s1}} w_{T_{s1}} \right)^2 + \left(\frac{\partial T_s}{\partial T_{s2}} w_{T_{s2}} \right)^2 + \left(\frac{\partial T_s}{\partial T_{s3}} w_{T_{s3}} \right)^2 \right]^{1/2} \tag{37}$$

Likewise, T_a is the mean of the values of the 16 air thermocouples ($T_{a1} - T_{a16}$) situated in the tested room:

$$T_a = \frac{(T_{a1} + T_{a2} + T_{a3} + \cdots + T_{a16})}{16} \tag{38}$$

$$w_{T_a} = \pm \left[\left(\frac{\partial T_a}{\partial T_{a1}} w_{T_{a1}} \right)^2 + \left(\frac{\partial T_a}{\partial T_{a2}} w_{T_{a2}} \right)^2 + \cdots + \left(\frac{\partial T_a}{\partial T_{a16}} w_{T_{a16}} \right)^2 \right]^{1/2} \tag{39}$$

Table 4 gives the results of uncertainty and expected errors for each experiment's measuring the convective, radiation, total HTCs, and heat fluxes.

The findings of the uncertainty analysis indicate that radiative HTC and heat-fluxes are of less uncertainty than those of other parameters because radiative HT is subtracted analytically using the Matlab© software. Since the measurement equipment had a relatively low sensitivity, the computed uncertainty values were modest. The uncertainties in the convection HTC and HT rate, however, were greater than those in the other variables because the subtraction of radiative HT from the total HT was used to determine the convection HT rate.

4. Results and discussion

Radiant wall heating and cooling applications come up with advantages such as being utilized in association with renewables, enabling a more favorable living environment thanks to lesser air movements, being retrofitted to existing structures, and practically

Table 4
The uncertainty results of experimental findings.

Parameter	1			2			3		
	Value	± w	w %	Value	± w	w %	Value	± w	w %
$\dot{q}_n$	72.49	2.6543	3.66	67.12	2.1626	3.22	59.77	1.6680	2.79
$\dot{q}_r$	50.74	0.0338	0.07	46.31	0.0340	0.07	41.24	0.0342	0.08
$\dot{q}_c$	21.75	1.8824	8.65	20.81	1.7134	8.23	18.53	1.5018	8.10
h_t	8.78	0.3431	3.91	8.58	0.3229	3.76	8.56	0.3255	3.80
h_r	6.06	0.0594	0.98	5.83	0.0601	1.03	5.76	0.0658	1.14
h_c	2.62	0.2280	8.70	2.64	0.2195	8.31	2.64	0.2159	8.18
Parameter	**4**			**5**			**6**		
	Value	**± w**	**w %**	**Value**	**± w**	**w %**	**Value**	**± w**	**w %**
$\dot{q}_n$	54.95	1.3621	2.48	50.24	1.2243	2.44	46.14	1.0734	2.33
$\dot{q}_r$	37.36	0.0343	0.09	33.66	0.0343	0.10	30.91	0.0347	0.11
$\dot{q}_c$	17.58	1.3637	7.76	16.58	1.2439	7.50	15.23	1.1408	7.49
h_t	8.48	0.3287	3.88	8.23	0.3340	4.06	7.88	0.3266	4.14
h_r	5.64	0.0699	1.24	5.45	0.0725	1.33	5.22	0.0721	1.38
h_c	2.69	0.2116	7.87	2.69	0.2055	7.64	2.58	0.1968	7.63
Parameter	**7**			**8**			**9**		
	Value	**± w**	**w %**	**Value**	**± w**	**w**	**Value**	**± w**	**w %**
$\dot{q}_n$	38.31	0.8813	2.30	34.35	0.7499	2.18	28.97	0.6093	2.10
$\dot{q}_r$	24.90	0.0253	0.10	22.33	0.0255	0.11	18.54	0.0255	0.14
$\dot{q}_c$	13.41	0.9428	7.03	12.02	0.8437	7.02	10.43	0.7104	6.81
h_t	7.16	0.3202	4.47	6.94	0.3294	4.75	7.07	0.3381	4.78
h_r	4.57	0.0680	1.49	4.42	0.0708	1.60	4.37	0.0837	1.91
h_c	2.47	0.1781	7.21	2.41	0.1738	7.21	2.49	0.1766	7.09
Parameter	**10**								
	Value	**± w**	**w %**						
$\dot{q}_n$	23.69	0.4711	1.99						
$\dot{q}_r$	14.92	0.0257	0.17						
$\dot{q}_c$	8.76	0.5842	6.67						
h_t	6.62	0.3206	4.83						
h_r	4.05	0.0895	2.21						
h_c	2.42	0.1707	7.06						

installation. Although those advantages result in indicated systems coming forward, a great number of factors affect the accurate determination of heating or cooling capacity. It should be noted that total, radiative, and convective HTCs at mostly confronted temperature differences are of major significance with regard to the precise determination of the capacity of those systems. The measured water inlet, radiant surface, and ambient temperatures as studied parameters were 10.05–20.10 °C, 17.63–23.12 °C, and 25.94–26.74 °C, respectively. The calculated values of studied parameters and their ranges can be clearly seen in Table 5. In this context, to precisely calculate the total HTC associated with those systems, with an accurate approach, convective and radiative HTCs which are an indispensable portion of thorough thermal performance analysis, must be revealed. Inaccurate determination of the thermal load of a living environment may arise from wrongly computed and applied HTCs in building energy simulations, leading to an excessive amount of energy consumption alongside the feeling of thermal discomfort.

Cooled surfaces of a living chamber are utilized to extract sensible heat firstly via thermal radiation dominantly and secondly by convection. The latter, whose subtype is natural convection, is caused by the temperature difference between the air temperature at the undisturbed regions of the flow inside the room and the surface temperature of the cooled radiant wall. A thoroughly implemented literature survey reveals that the sophisticated nature of convection HT requires further experimental findings to be obtained to understand the HT characteristics of an enclosure equipped with cooled radiant surfaces, whereas, mathematical models are quite adequate to calculate the conductive and radiative HT phenomena.

Those cooling systems are able to address thermal comfort requirements under summer conditions by comparatively higher indoor air temperatures due to the fact that an overwhelming portion of cooling loads can be met by extracting sensible heat by means of radiative HT with peers and bodies instead of air. When persons, bodies, and walls in living environments absorb thermal radiation their temperature increases. So long as temperatures of those given before are higher than the cooled radiant surfaces, heat will be transferred from them to the cooled surfaces. Convection acts as a way of HT since air particles touching the cooled surfaces will get cooled. In case the environment is of a humid behavior, the latent loads should be removed using a discrete auxiliary system, on the other hand, hot and dry climates having a large ratio of cooling via disposing of sensible heat are so convenient for utilization of radiant cooling systems.

Obtained data, such as indoor air temperatures, surface temperatures, and calculated outputs, that are heat fluxes, HTCs, operative temperature, and average area-weighted temperature of unconditioned surfaces, are presented in Table 5 as a result of 10 individual conducted experiments. As demonstrated in Table 5, the experimental measurements and results corresponding to HT characteristics of a cooled vertical wall in a living environment that were mentioned in previous lines, are presented. Those case studies consisting of 10 individual tests obtained under different thermal boundary conditions are elaborated in this table. Throughout the tests, supply water temperatures and surface temperatures of the cooled vertical wall, which may be defined as thermal boundary conditions of the HT problem, lie within the ranges of 10.05–20.10 °C and 17.63–23.12 °C, correspondingly. One should be aware of the fact that, in the cooling process, what matters is that

Table 5
Experimentally obtained and calculated values.

Experimental Cases		1	2	3	4	5	6	7	8	9	10
T_w	(°C)	10.05	10.82	11.98	13.05	14.12	14.98	16.46	17.41	19.04	20.10
T_s	(°C)	17.63	18.13	19.02	19.66	20.18	20.46	21.08	21.53	22.47	23.12
T_a	(°C)	25.94	26	26.05	26.19	26.33	26.36	26.50	26.52	26.66	26.74
T_{op}	(°C)	25.89	25.95	26.00	26.14	26.28	26.32	26.43	26.48	26.56	26.70
T_{AUST}	(°C)	26.0	26.08	26.19	26.28	26.35	26.39	26.53	26.59	26.71	26.80
Q_t	(W)	917	834	730	662	603	552	457	408	342	279
Q_g	(W)	120	96	72	57	51	44	36	30	24	18
Q_n	(W)	797	738	657	604	553	508	421	378	319	261
Q_r	(W)	558	509	454	411	370	340	274	246	204	164
Q_c	(W)	239	229	204	193	182	167	147	132	115	96
$\dot{q}_t$	(W/m^2)	83.36	75.85	66.34	60.17	54.86	50.15	41.57	37.10	31.11	25.34
$\dot{q}_g$	(W/m^2)	10.87	8.73	6.57	5.22	4.62	4.01	3.26	2.75	2.14	1.66
$\dot{q}_n$	(W/m^2)	72.49	67.12	59.77	54.95	50.24	46.14	38.31	34.35	28.97	23.69
$\dot{q}_r$	(W/m^2)	50.74	46.31	41.24	37.36	33.66	30.91	24.90	22.33	18.54	14.92
$\dot{q}_c$	(W/m^2)	21.75	20.81	18.53	17.58	16.58	15.23	13.41	12.02	10.43	8.76
$T_{op} - T_s$	(°C)	8.26	7.82	6.98	6.48	6.11	5.85	5.35	4.95	4.09	3.58
$T_{AUST} - T_s$	(°C)	8.37	7.95	7.17	6.62	6.17	5.93	5.45	5.05	4.24	3.68
$T_a - T_s$	(°C)	8.31	7.87	7.03	6.53	6.16	5.90	5.42	4.99	4.19	3.62
h_t	(W/m^{2}K)	8.78	8.58	8.56	8.48	8.23	7.88	7.16	6.94	7.07	6.62
h_r	(W/m^{2}K)	6.06	5.83	5.76	5.64	5.45	5.22	4.57	4.42	4.37	4.05
h_c	(W/m^{2}K)	2.62	2.64	2.64	2.69	2.69	2.58	2.47	2.41	2.49	2.42

the radiant cooling application runs with an average temperature higher than the dew point temperature. In general, relying on the necessities and outdoor weather (the outside temperature and relative humidity of air), the radiant cooled surface temperature must be a minimum of 16 °C. To prevent condensation on cooled surfaces it should be provided the temperature of the cooled surface does not fall drop under 16 °C. Also, the average air temperature in the chamber varies in the interval of 25.94–26.74 °C. Apart from most of the relevant literature, in the current radiant cooling investigation heat gains from the back surface of the experimental chamber by conduction were paid attention to, whose heat fluxes spanned from 1.66 to 10.87 W/m^2. Net heat flux extracted from the surrounding surfaces of the room and room air was acquired by subtracting the heat fluxes gained through the back surface of the examined panel from the total heat flux, whose range encompasses between 23.69 and 72.49 W/m^2. Radiative and convective heat fluxes that compose net heat fluxes change within the ranges of 14.92–50.74 W/m^2 and 8.76–21.75 W/m^2, respectively.

HTCs over an examined surface that are a measure of different types of HT mechanisms which also reflect the magnitude of HT rate per square meter per temperature difference between surface temperature and the reference temperature valid for corresponding HT mechanism, were presented in this table. It was revealed that total, radiative, and convective HTCs over a radiant vertical cooled wall included in a living chamber appeared in the intervals of 6.62–8.78, 4.05–6.06, and 2.41–2.62 W/m^{2}K, respectively.

Fig. 10 illustrates the alteration of total heat fluxes according to the temperature difference between operative temperature and cooled wall surface temperature, and as expectedly, it is seen that total heat flux increases with growing temperature differences. Findings through the experiments were depicted in the figure and an inclination line was drawn to disclose the total heat flux behavior of such a system. Also, it should be emphasized that as the supply water temperature decreased as could be observed from Table 5, the total heat flux increased because the corresponding temperature difference was ($T_{op} - T_s$), ascended. To validate, total heat flux results were compared with the results from the total heat flux equation given in the standard EN1264 [30] and EN15377 [29]. It was noticed that the outcomes of the present investigation deviated from the equation given by those standards by ± 15 % which is a quite tolerable band. By the temperature difference of 6 °C, this equation is over-predicted, and from 6 °C forward the equation underestimated the results. This may possibly be attributed to temperature differences under which the equation from the standard was derived to be roughly around 6 °C. Additionally, an equation, which is valid for a quite extensive temperature difference range, for total heat flux to a cooled radiant wall taking place in a living chamber of dimensions very close to a real-sized chamber whose surroundings were entirely conditioned to actual environmental conditions, were proposed in Eq. (40). The mean square error of proposed equation was found to be 0.99, that is a highly trustable value. In building energy simulation programs and by researchers in this field, the proposed equation with its wide temperature difference interval can be utilized and contribute to reaching better thermal comfort and diminishing energy consumption.

$$q_t = 8.2(T_{op} - T_s) \tag{40}$$

Fig. 11 indicates the variation of the radiation heat fluxes with respect to corresponding temperature differences ($T_{AUST} - T_S$), showing that increase in this value results in a rise in radiative heat fluxes, as expectedly. Furthermore, a trendline taking entire results into consideration was drawn as can be seen in the figure, and a correlation associated with this trendline having a mean square error of 0.98, was suggested in Eq. (41). As discussed in the interpretation of total heat flux results in Fig. 10, by the temperature difference of 6 °C the correlation overpredicted the radiative heat fluxes while as of 6 °C the correlation underestimated those values.

$$q_r = 5.4(T_{AUST} - T_s) \tag{41}$$

Fig. 12 represents the alteration of convection heat fluxes according to temperature differences (T_a-T_s) and a comparison with the ASHRAE [37]. It is observed that with increasing temperature differences convection heat fluxes ascend almost linearly because of stronger natural convection currents led by density differences between the air in contact with the cooled surface and the room air. Additionally, different from the tendencies of total and radiative heat fluxes with respect to corresponding temperature differences, no significant overestimation and underestimation

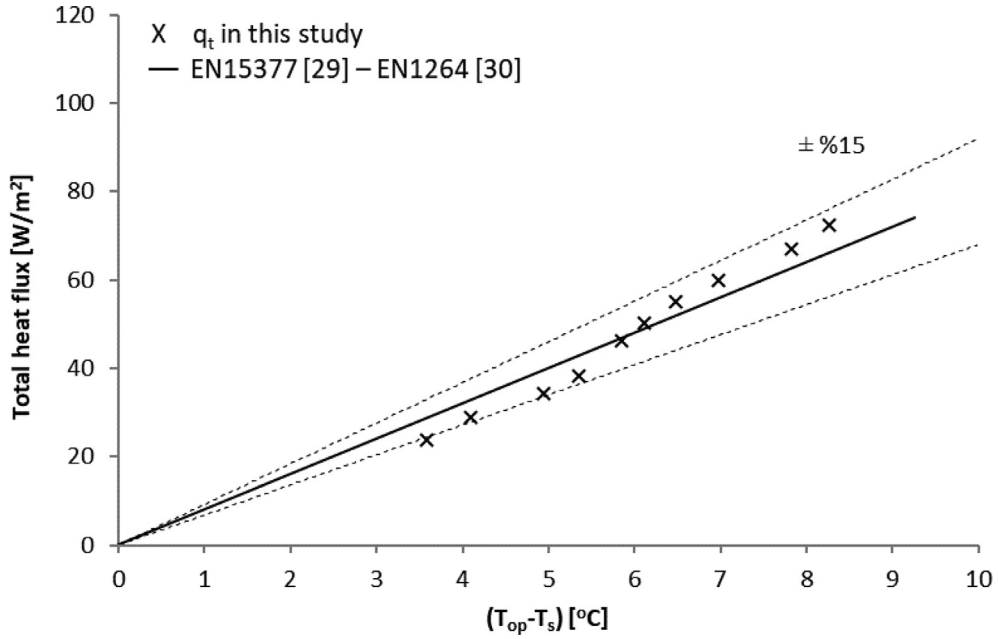


Fig. 10. Variation of total heat fluxes with respect to corresponding temperature differences and comparison with the standards EN15377 [29] and EN1264 [30].

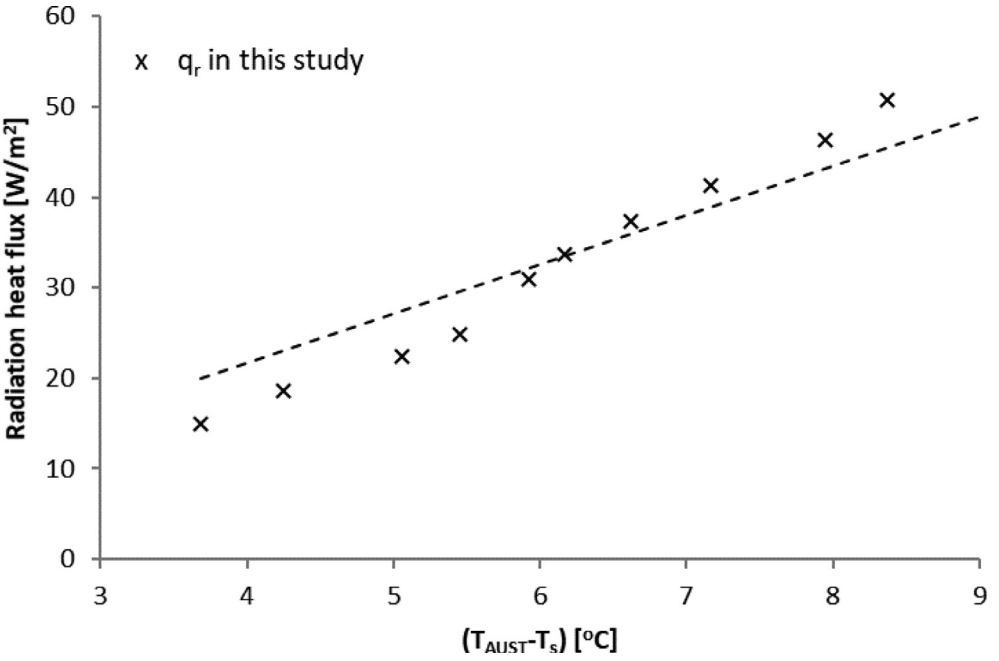


Fig. 11. Variation of radiation heat fluxes with respect to corresponding temperature differences.

are discerned up to 6 °C and beginning from 6 °C, respectively. The correlation provided by ASHRAE [37] was implemented to contrast the results of the current work with regard to convective heat flux findings. It is quite noticeable that the outcomes of the correlation of ASHRAE [37] slightly underestimate the outcomes of the current investigation. These differences can be clarified by the temperature difference range, under which ASHRAE's [37] tests were conducted, the examined panel types, and whether heat gains from the back surface of the examined panel were considered or not. A convective heat flux correlation for a radiant cooled wall was developed and given in Eq. (42), having a mean squared error value of 0.99.

$$q_c = 2.6(T_a - T_s) \tag{42}$$

Fig. 13 illustrates the ratios of the components of the total HT rate. Regarding the presentation, 67 % and 33 % of the total HT averagely belonged to the radiative and convective HT in the case of radiant cooling wall application, respectively. Moreover, the rate

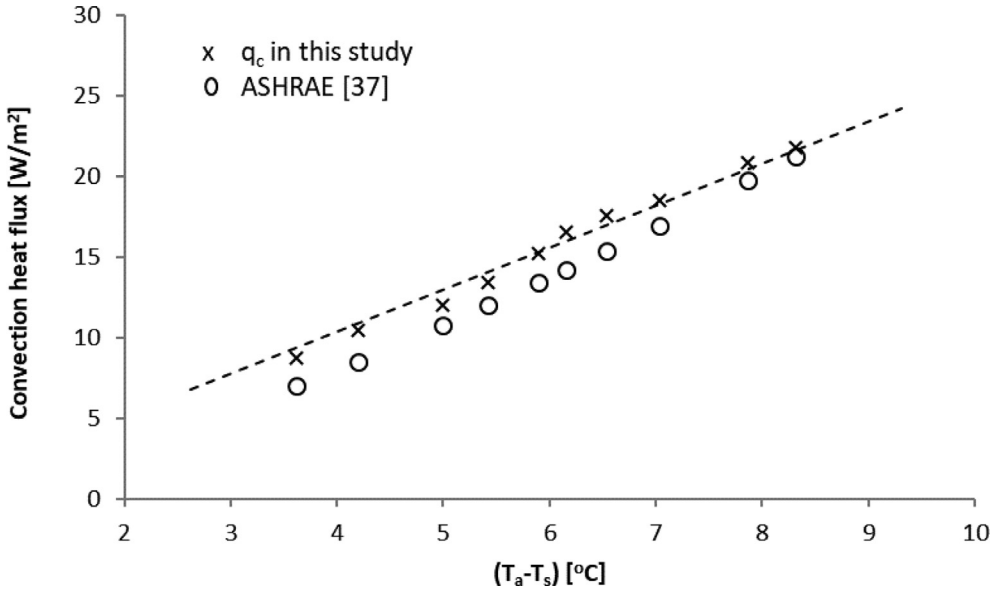


Fig. 12. Variation of convection heat fluxes with respect to corresponding temperature differences and comparison with the ASHRAE [37].

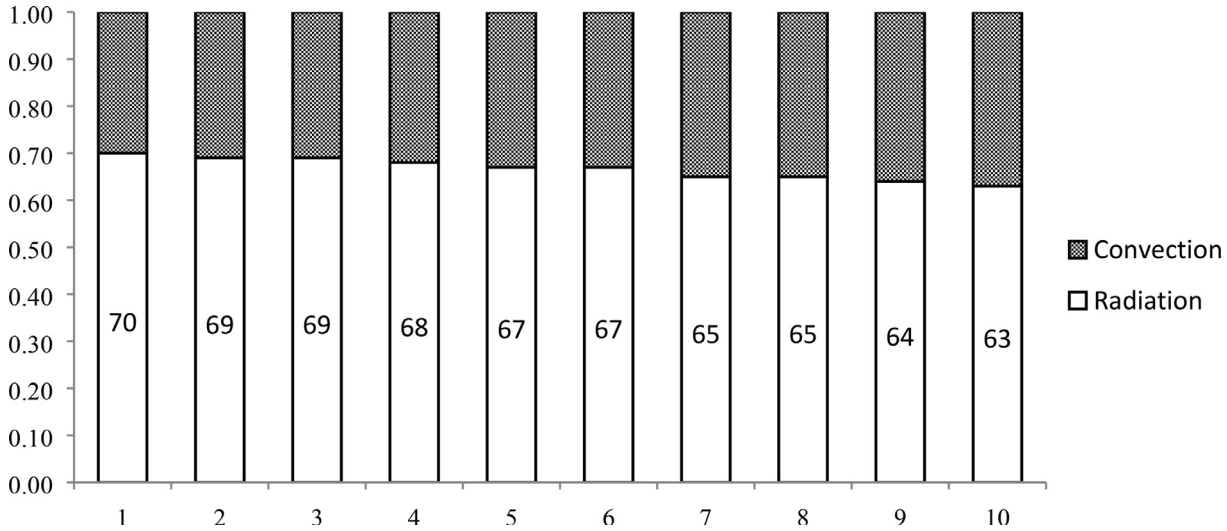


Fig. 13. The proportion of radiative heat transfer to total heat transfer through a radiant cooled wall.

of radiative HT was calculated in the interval of 63 and 70 %. It should be noted that the data used in this figure also exist in Table 5. The ratios on this figure decrease gradually with increasing supply water temperature, in other words, radiant wall surface temperature, as expected. The tendency existing in this figure is due to the reduction in temperature difference, ($T_{aust} - T$), in Eq. (5) through the experiments from 1 to 10 related to the calculation of radiative HT component.

Fig. 14 illustrates the alteration of total, radiative, and convective HTCs by test number. As the vertical cooled radiant surface temperature increased as a result of increasing supply water temperatures, HTCs decreased, as well. One can notice from the figure that, the average total, radiative, and convective HTCs lie within the intervals of 6.62–8.78, 4.05–6.06, and 2.41–2.62 W/m^{2}K, respectively. As stated in Fig. 13, radiative HT was dominant on the total one, for that reason, total HTCs decreased with decreasing radiative one. Finally, according to the literature review, all calculated HTCs in this figure, which were 7.83, 5.14, and 2.57 W/m^{2}K averagely, were realized to be consistent with those in the literature and standards. In this context, EN 15377 [29], EN 1264 [30], and REHVA [4] standards proposed a total HTC of 8 W/m^{2}K for radiant wall heating and cooling applications. In addition, Acikgoz and Kincay [42] and Koca [43] offered the total HTCs of 8.1 and 8.25 W/m^{2}K according to their experimental radiant cooled wall analyses, respectively. Regarding the radiative HTC values of radiant heated/cooled walls, EN 15377 [29] and EN 1264 [30] suggested the value of 5.5 W/m^{2}K, Acikgoz and Kincay [42] and Koca [43] proposed the coefficients of 4.3 and 5.52 W/m^{2}K, in turn. Concerning the convective HTC of radiant cooled walls, Acikgoz and Kincay [42] and Koca [43] offered values of 2.7 and 2.41 W/m^{2}K, correspondingly. It should be noted that there is no revealed convective HTC by standards pertaining to radiant cooled walls.

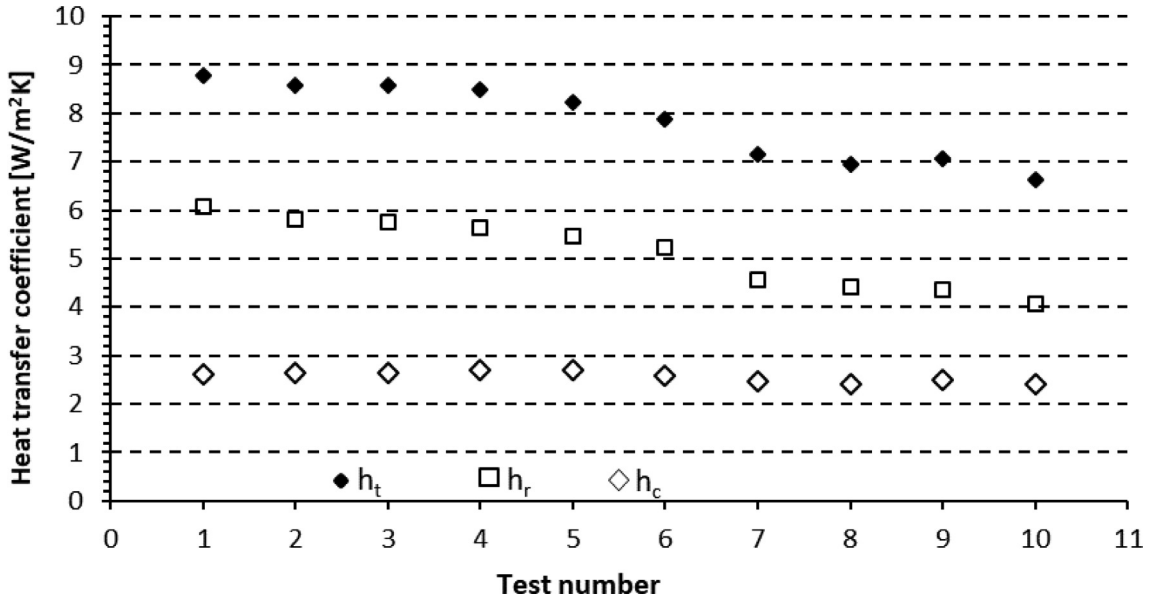


Fig. 14. Variation of total, radiative, and convective HTCs with respect to corresponding test number.

5. Conclusion

Although radiant heating and cooling applications are frequently employed in residential and commercial structures, there exist gaps, that directly affect energy consumption, such as a better accuracy in the determination of HT rates in the planning period to be achieved. Unlike the vast majority of the existing investigations concerned with using the floor and ceiling as a heat sink or gain source for radiant applications, the walls have benefitted to condition the indoor environment in the present study. Besides, the room size is a significant criterion in terms of reliability and consistency of proposed correlations and coefficients, for that reason, the test chamber has actual dimensions different from most of the other studies. In addition, the current work is the third experimental one as the radiant wall cooling application to determine the HT characteristics in a real-sized living environment. It should be noted that the prior two works on the same subject belong to the same research group. Furthermore, whole essential elements, such as reference temperature determination and HT calculation method, are given in detail for the sake of readers. Outcomes derived from this practical study can be summed up with the following points:

a. Referring HT characteristics pertaining to a radiant cooled wall taking place within a real-sized room, experimental measurements and results have been contributed to the relevant literature.
b. Heat transmitted from the rear surface of the examined cooled surface encompassing the heat flux range of 1.66–10.87 W/m^2 has been taken into account differently from most of the relevant investigations.
c. The Net heat flux range absorbed from the surrounding surface and the room air lies between 23.69–72.49 W/m^2. Moreover, radiative and convective heat fluxes that make up the net total heat flux are found to be lying in the intervals of 14.92–50.74 W/m^2 and 8.76–21.75 W/m^2, respectively.
d. The intervals, 6.62–8.78, 4.05–6.06, and 2.41–2.62 W/m^{2}K, corresponding to total, radiative, and convective HTCs associated with a cooled wall in a real-sized living environment, have been acquired, respectively.
e. The heat flux equation provided by well-known international standards has been utilized to verify the outcomes of the current work and noticed that the results differentiated by ±15 %.
f. A total heat flux correlation spanning an extensive temperature difference range ($T_{op} - T_s$) has been suggested whose mean square error is 0.99.
g. The alteration of the radiative heat fluxes according to the temperature differences ($T_{AUST} - T_S$), demonstrates that an increase in this value leads to an augmentation in radiative heat fluxes, and an equation revealing this behavior having a mean square error of 0.98, has been proposed.
h. An equation for the determination of convective heat flux for a radiant cooled wall has been produced whose mean squared error value is 0.99.
i. 67 % and 33 % of the total HT in average have been found to be corresponding to radiative and convective HT when the case is a radiant wall cooling application.
j. For the utilization of engineers and researchers in the field of building energy simulation, total, radiative, and convective HTCs of 7.83, 5.14, and 2.57 W/m^{2}K, have been proposed for a radiant wall cooling application in a living chamber, respectively.

Data availability

Data will be made available on request.

Declaration of Competing Interest

The authors declare that they have no known competing financial interests or personal relationships that could have appeared to influence the work reported in this paper.

Acknowledgments

This work was financially funded by the Scientific and Technological Research Council of Turkey (TUBITAK) via the TEYDEB-1507 (3100577) and ARDEB-3001 (213M199) projects, which were coordinated by Dr. Koca. The experiments were carried out at the Mir Arastirma and Gelistirme A.S. company facilities.

References

[1] M.W. Ahmad, M. Mourshed, Y. Rezgui, Trees vs Neurons: Comparison between random forest and ANN for high-resolution prediction of building energy consumption, Energy Build. 147 (2017) 77–89, https://doi.org/10.1016/j.enbuild.2017.04.038.

[2] IEA, Tracking buildings, Paris, France, 2020. https://www.iea.org/reports/tracking-buildings-2020.

[3] J. Ngarambe, G.Y. Yun, M. Santamouris, The use of artificial intelligence (AI) methods in the prediction of thermal comfort in buildings: energy implications of AI-based thermal comfort controls, Energy Build. 211 (2020), https://doi.org/10.1016/j.enbuild.2020.109807.

[4] B. J., O. B.W., P. D., REHVA Guidebook No. 7 – Low temperature heating and high temperature cooling, REHVA, 2007.

[5] A. Hesaraki, N. Huda, A comparative review on the application of radiant low-temperature heating and high-temperature cooling for energy, thermal comfort, indoor air quality, design and control, Sustain. Energy Technol. Assessments. 49 (2022), https://doi.org/10.1016/j.seta.2021.101661.

[6] Y. Karakoyun, O. Açikgöz, A.S. Dalkiliç, Z. Yumurtaci, An experimental investigation on radiant floor heating systems at various operating conditions, J. Therm. Eng. 6 (2020), https://doi.org/10.18186/THERMAL.799427.

[7] O. Acikgoz, Y. Karakoyun, Z. Yumurtacı, N. Dukhan, A.S. Dalkılıç, Realistic experimental heat transfer characteristics of radiant floor heating using sidewalls as heat sinks, Energy Build. 183 (2019), https://doi.org/10.1016/j.enbuild.2018.11.022.

[8] H.E. Feustel, C. Stetiu, Hydronic radiant cooling – preliminary assessment, Energy Build. 22 (1995) 193–205, https://doi.org/10.1016/0378-7788(95)00922-K.

[9] W. Zeiler, G. Boxem, Effects of thermal activated building systems in schools on thermal comfort in winter, Build. Environ. 44 (2009) 2308–2317, https://doi.org/10.1016/j.buildenv.2009.05.005.

[10] T. Imanari, T. Omori, K. Bogaki, Thermal comfort and energy consumption of the radiant ceiling panel system, Energy Build. 30 (1999) 167–175, https://doi.org/10.1016/s0378-7788(98)00084-x.

[11] M. Al-Othmani, K. Ghali, N. Ghaddar, Experimental and theoretical study of transient human thermal comfort response in convective and radiative environments, HVAC R Res. 15 (2009) 855–873, https://doi.org/10.1080/10789669.2009.10390869.

[12] Q. Chen, Comfort and energy consumption analysis in buildings with radiant panels, Energy Build. 14 (1990) 287–297, https://doi.org/10.1016/0378-7788(90)90091-V.

[13] C. Stetiu, Energy and peak power savings potential of radiant cooling systems in US commercial buildings, Energy Build. 30 (1999) 127–138, https://doi.org/10.1016/S0378-7788(98)00080-2.

[14] R.A. Memon, S. Chirarattananon, P. Vangtook, Thermal comfort assessment and application of radiant cooling: a case study, Build. Environ. 43 (2008) 1185–1196, https://doi.org/10.1016/j.buildenv.2006.04.025.

[15] J. Oravec, O. Šikula, M. Krajčík, M. Arıcı, M. Mohapl, A comparative study on the applicability of six radiant floor, wall, and ceiling heating systems based on thermal performance analysis, J. Build. Eng. 36 (2021), https://doi.org/10.1016/j.jobe.2020.102133.

[16] P. Vangtook, S. Chirarattananon, An experimental investigation of application of radiant cooling in hot humid climate, Energy Build. 38 (2006) 273–285, https://doi.org/10.1016/j.enbuild.2005.06.022.

[17] M. Krajčík, M. Arıcı, O. Šikula, M. Šimko, Review of water-based wall systems: heating, cooling, and thermal barriers, Energy Build. 253 (2021), https://doi.org/10.1016/j.enbuild.2021.111476.

[18] H. Karabay, M. Arici, M. Sandik, A numerical investigation of fluid flow and heat transfer inside a room for floor heating and wall heating systems, Energy Build. 67 (2013) 471–478, https://doi.org/10.1016/j.enbuild.2013.08.037.

[19] J.A. Myhren, S. Holmberg, Flow patterns and thermal comfort in a room with panel, floor and wall heating, Energy Build. 40 (2008) 524–536, https://doi.org/10.1016/j.enbuild.2007.04.011.

[20] T. Mikeska, J. Fan, S. Svendsen, Full scale measurements and CFD investigations of a wall radiant cooling system integrated in thin concrete walls, Energy Build. 139 (2017) 242–253, https://doi.org/10.1016/j.enbuild.2017.01.033.

[21] M. Krajčík, M. Šimko, O. Šikula, D. Szabó, D. Petráš, Thermal performance of a radiant wall heating and cooling system with pipes attached to thermally insulating bricks, Energy Build. 246 (2021), https://doi.org/10.1016/j.enbuild.2021.111122.

[22] T. Mikeska, S. Svendsen, Dynamic behavior of radiant cooling system based on capillary tubes in walls made of high performance concrete, Energy Build. 108 (2015) 92–100, https://doi.org/10.1016/j.enbuild.2015.08.050.

[23] P. Vangtook, S. Chirarattananon, Application of radiant cooling as a passive cooling option in hot humid climate, Build. Environ. 42 (2007) 543–556, https://doi.org/10.1016/j.buildenv.2005.09.014.

[24] J. Romaní, G. Pérez, A. de Gracia, Experimental evaluation of a cooling radiant wall coupled to a ground heat exchanger, Energy Build. 129 (2016) 484–490, https://doi.org/10.1016/j.enbuild.2016.08.028.

[25] M. Bojić, D. Cvetković, L. Bojić, Decreasing energy use and influence to environment by radiant panel heating using different energy sources, Appl. Energy. 138 (2015) 404–413, https://doi.org/10.1016/j.apenergy.2014.10.063.

[26] J. Romaní, G. Pérez, A. de Gracia, Experimental evaluation of a heating radiant wall coupled to a ground source heat pump, Renew. Energy. 105 (2017) 520–529, https://doi.org/10.1016/j.renene.2016.12.087.

[27] M. Krzaczek, J. Florczuk, J. Tejchman, Improved energy management technique in pipe-embedded wall heating/cooling system in residential buildings, Appl. Energy. 254 (2019), https://doi.org/10.1016/j.apenergy.2019.113711.

[28] U. Akbulut, O. Kincay, Z. Utlu, Analysis of a wall cooling system using a heat pump, Renew. Energy. 85 (2016) 540–553, https://doi.org/10.1016/j.renene.2015.07.005.

[29] EN15377-1: Heating Systems in Buildings – Design of Embedded Water Based Surface Heating and Cooling Systems – Part 1: Determination of the Design Heating and Cooling Capacity, CEN, 2008.

[30] EN1264-5: Water Based Surface Embedded Heating and Cooling Systems – Part 5: Heating and Cooling Surfaces Embedded in Floors, Ceilings and Walls - Determination of the Thermal Output, CEN, 2008.

[31] A. Koca, Z. Gemici, Y. Topacoglu, G. Cetin, R.C. Acet, B.B. Kanbur, Experimental investigation of heat transfer coefficients between hydronic radiant heated wall and room, Energy Build. 82 (2014) 211–221, https://doi.org/10.1016/j.enbuild.2014.06.045.

[32] A. Koca, Experimental examination of heat transfer performance of the heated radiant wall system, J. Therm. Eng. 4 (2018) 2394–2407, https://doi.org/10.18186/thermal.465641.

[33] O. Acikgoz, A. Çebi, A.S. Dalkilic, A. Koca, G. Çetin, Z. Gemici, S. Wongwises, A novel ANN-based approach to estimate heat transfer coefficients in radiant wall heating systems, Energy Build. 144 (2017) 401–415, https://doi.org/10.1016/j.enbuild.2017.03.043.

[34] ASHRAE, 2012 ASHRAE Handbook Heating, Ventilating, and Air-Conditioning Systems and Equipment, Atlanta GA, 2012.

[35] F. Alamdari, G.P. Hammond, Improved data correlations for buoyancy-driven convection in rooms, Build. Serv. Eng. Res. Technol. 4 (1983) 106–112, https://doi.org/10.1177/014362448300400304.

[36] S.W. Churchill, H.H.S. Chu, Correlating equations for laminar and turbulent free convection from a vertical plate, Int. J. Heat Mass Transf. 18 (1975) 1323–1329, https://doi.org/10.1016/0017-9310(75)90243-4.

[37] ASHRAE, HVAC Systems and Equipment Handbook, Chapter 6: Panel Heating and Cooling, 2016.

[38] H.B. Awbi, A. Hatton, Natural convection from heated room surfaces, Energy Build. 30 (1999) 233–244, https://doi.org/10.1016/S0378-7788(99)00004-3.

[39] A.J.N. Khalifa, R.H. Marshall, Validation of heat transfer coefficients on interior building surfaces using a real-sized indoor test cell, Int. J. Heat Mass Transf. 33 (1990) 2219–2236, https://doi.org/10.1016/0017-9310(90)90122-B.

[40] O. Acikgoz, A novel evaluation regarding the influence of surface emissivity on radiative and total heat transfer coefficients in radiant heating systems by means of theoretical and numerical methods, Energy Build. 102 (2015) 105–116, https://doi.org/10.1016/j.enbuild.2015.05.016.

[41] J. Shinoda, O.B. Kazanci, S. Tanabe, B.W. Olesen, A review of the surface heat transfer coefficients of radiant heating and cooling systems, Build. Environ. 159 (2019), https://doi.org/10.1016/j.buildenv.2019.05.034.

[42] O. Acikgoz, O. Kincay, Experimental and numerical investigation of the correlation between radiative and convective heat-transfer coefficients at the cooled wall of a real-sized room, Energy Build. 108 (2015) 257–266, https://doi.org/10.1016/j.enbuild.2015.09.013.

[43] A. Koca, Experimental examination of heat transfer coefficients in hydronic radiant wall cooling systems, J. Build Eng. (2022).

[44] CEN, BS EN 14037-5:2016 Free hanging heating and cooling surfaces for water with a temperature below 120°C Open or closed heated ceiling surfaces. Test method for thermal output, 2016.

[45] M. de C. B.W. Olesen, F. Bonnefoi, E. Michel, Heat exchange coefficient between floor surface and space by floor cooling – Theory or a question of definition, ASHRAE Trans. (2000).

[46] A. Koca, Ö. Atayılmaz, Ö. Ağra, Numerical and experimental examinations of free convection condensation of steam in the presence of air over the cooled panel, Energy Build. 269 (2022), https://doi.org/10.1016/j.enbuild.2022.112250.

[47] ASHRAE, ANSI/ASHRAE 138-2021 Standard Method of Testing For Rating Ceiling Panels For Sensible Heating And Cooling, 2021.

[48] A. Koca, Ö. Atayılmaz, Ö. Ağra, Experimental investigation of heat transfer and dehumidifying performance of novel condensing panel, Energy Build. 129 (2016) 120–137, https://doi.org/10.1016/j.enbuild.2016.07.049.

[49] ASHRAE, ANSI/ASHRAE Standard 55-2020: Thermal Environmental Conditions for Human Occupancy, 2020.

[50] DIN, DIN EN 14240 Standard: Ventilation for buildings - Chilled ceilings - Testing and rating, 2004.

[51] K.S.C.R.D. Watson, Radiant Heating and Cooling Handbook, McGraw-Hill, 2002.

[52] J.P. Holman, Experimental Methods for Engineers, McGraw-Hill Inc, New York, 2012.